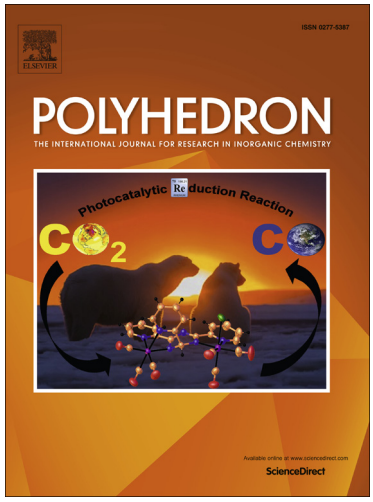

Unusual octahedral Hg(II) dithiocarbamate : Synthesis, spectral and structural studies on Hg(II) complexes with pyrrole based dithiocarbamates and their utility for the preparation of α- and β-HgS

Govindasamy Gurumoorthy, Subbiah Thirumaran, Samuele Ciattini

PII: S0277-5387(16)30360-6
DOI: http://dx.doi.org/10.1016/j.poly.2016.08.001
Reference: POLY 12138

To appear in: *Polyhedron*

Received Date: 1 July 2016
Revised Date: 30 July 2016
Accepted Date: 2 August 2016

Please cite this article as: G. Gurumoorthy, S. Thirumaran, S. Ciattini, Unusual octahedral Hg(II) dithiocarbamate : Synthesis, spectral and structural studies on Hg(II) complexes with pyrrole based dithiocarbamates and their utility for the preparation of α- and β-HgS, *Polyhedron* (2016), doi: http://dx.doi.org/10.1016/j.poly.2016.08.001

Unusual octahedral Hg(II) dithiocarbamate : Synthesis, spectral and structural studies on Hg(II) complexes with pyrrole based dithiocarbamates and their utility for the preparation of α- and β-HgS

Govindasamy Gurumoorthy[a], Subbiah Thirumaran[a*] and Samuele Ciattini[b]

[a]Department of Chemistry, Annamalai University, Annamalainagar- 608 002, India.

[b]Centro di Cristallografia Strutturale, Polo Scientifio di Sesto Fiorentino, Via della Lastruccia No. 3, 50019 Sesto Fiorentino, Firenze, Italy

Correspondence e-mail: sthirumaran@yahoo.com

***Corresponding author**
Dr. S. Thirumaran
Department of Chemistry
Annamalai University
Annamalainagar 608 002
Tamil Nadu, INDIA
Tel: +91 9842897597
E-mail: sthirumaran@yahoo.com

Unusual octahedral Hg(II) dithiocarbamate : Synthesis, spectral and structural studies on Hg(II) complexes with pyrrole based dithiocarbamates and their utility for the preparation of α- and β-HgS

Govindasamy Gurumoorthy[a], Subbiah Thirumaran[a*] and Samuele Ciattini[b]

[a]Department of Chemistry, Annamalai University, Annamalainagar- 608 002, India.

[b]Centro di Cristallografia Strutturale, Polo Scientifio di Sesto Fiorentino, Via della Lastruccia No. 3, 50019 Sesto Fiorentino, Firenze, Italy

Correspondence e-mail: sthirumaran@yahoo.com

Abstract

Bis(N-(pyrrol-2-ylmethyl)-N-butyldithiocarbamato-S,S′)mercury(II) (**1**) and bis(N-(pyrrol-2-ylmethyl)-N-(2-phenylethyl)dithiocarbamato-S,S′)mercury(II)(**2**) were prepared and characterized by microanalysis, spectroscopy (IR, ^{1}H and ^{13}C NMR) and their structures were elucidated by X-ray crystallography. Complexes **1** and **2** exist as monomer and polymer, respectively. The central mercury atom in **1** is asymmetrically chelated by two dithiocarbamate ligands leading to a distorted tetrahedral geometry. In complex **2**, the mercury is six coordinate with distorted octahedral coordination geometry. In this case, both dithiocarbamate ligands function as bridging triconnective ligand. This indicates that small changes in R groups of dithiocarbamate ligand gave different structures. Complexes **1** and **2** were used as single source precursors for the preparation of mercury sulfide nanoparticles. Mercury sulfides were characterized by XRD, TEM, EDAX, IR, UV and fluorescence spectra. Solvothermal decomposition of **1** yielded three different morphological (hexagonal, cube and spherical) α- mercury sulfide nanoparticles and **2** gave only spherical β- mercury sulfide nanoparticles.

1.Introduction

Mercury(II) dithocarbamate complexes have been extensively studied because of their wide biological, industrial , agricultural and chemical applications [1-5]. Dithiocarbamate ligands display a variety of coordination patterns such as monodentate, bidentate (isobidentate or anisobidentate in chelating and bridging situations), triconnective *etc.,* leading to a great diversity of molecular and supramolecular structures [6]. Particularly, six different coordination motifs have been observed for mercury(II) dithiocarbamates (**scheme-1**) [7]. There are two mononuclear motifs (I and II). Motifs I and II feature a grossly distorted tetrahedral geometry [8] and a square planar geometry [9], respectively about the central atom. Dimeric motifs fall in to two distinct classes (motifs III and IV). These motifs are found that feature two chelating and two bridging dithiocarbamate ligands. The only difference between the motifs III and IV relates to the relative disposition of the bridging dithiocarbamate ligands ie., in motif III they lie to the same side of the dimer[10] but for motif IV they lie in opposite sides[11]. The eight membered ring in structural motifs III and IV can be described as a saddle and twisted chair conformations, respectively. Trimeric motif (V) is found in $[Hg_3(thqdtc)_6]$.py (thqdtc=1,2,3,4-tetrahydroquinoline carbodithioate)[12]. In this motif the environments of two mercury atoms are similar (five coordinated) but their environments are different from another mercury atom (four coordinated). Finally there is one example of motif VI (layer structure) *i.e.* for $Hg(S_2CNH_2)_2$ [13]. In this case all dithiocarbamate ligands are bridging and each mercury atom exists in a distorted tetrahedral geometry. Based on systematic studies of series of structures where the only difference between them is in the nature of N-bound organic moiety, it has been concluded that the actual structure adopted in Hg(II) dithiocarbamate complexes is dependant of the N-bound organic moiety. This may be utilized as a design element in crystal engineering

especially in main group elements [6]. In addition to the structural properties, mercury(II) dithiocarbamate complexes have been used as single source precursors for the preparation of mercury sulfide nanoparticles [14-16]. Suitable changes in the organic moiety of dithiocarbamate ligands can affect the phase and morphology of the metal sulfide nanoparticles [17]. Various size and shape of mercury sulfide nanoparticles have a wide range of applications such as ultrasonic transducers, image sensor, electrostatic image materials, flat-panel devices, photoelectric conversion devices, non-linear optical material and solar cells [18-24]. Due to the interesting structural variations of Hg(II) dithiocarbamate complexes and their utilization to prepare various size and shape of mercury sulfide nanoparticles, herein we report synthesis, spectral and structural studies on complexes **1** and **2** and preparation of mercury sulfide nanoparticles from both the complexes.

2. Experimental

2.1 Materials and techniques

All chemicals were of analytical grade obtained from commercial sources and used without further purification. IR spectra were recorded on a Thermo Nicolet Avatar 330 FT-IR spectrophotometer (range: 4000–400 cm^{-1}) as KBr pellets. The ^{1}H and ^{13}C NMR spectra were recorded on BRUKER 400/100 MHz NMR spectrometer at room temperature in $CDCl_3$ solvent. PXRD and TEM images were performed using EQUINX 1000 and TECNAI T2 G2 make-FEI, respectively. EDS were performed by SUPRA 55VP CARL. A Shimadzu UV-1650 PC double-beam UV-vis spectrophotometer was used for recording the electronic spectra. Fluorescence spectra were recorded using Perkin Elmer 1555 fluorescence spectrophotometer at room temperature.

2.2. X-ray crystallography

Diffraction data were recorded on Xcalibur, Sapphire3 diffractometer using graphite-monochromated MoKα radiation (λ= 0.71073 Å) at an ambient temperature. The structure was solved by SHELXS 97 [25] and refined by full-matrix least square methods in SHELXL-97 [26]. All non-hydrogen atoms were refined anisotropically and the hydrogen atoms were refined isotropically. Details of the crystal data and structure refinement parameters for **1** and **2** are summarized in Table **1**.

2.3. Computational study

The HOMO–LUMO energies was calculated with Gaussian 03 software package using gradient-corrected DFT with the B3LYP functional, in which the LanL2DZ basis set was used by including effective core potential functions [27].

2.4. Preparation of complexes

2.4.1.Preparation of amines

N-(pyrrol-2-ylmethyl)-N-butylamine and N-(pyrrol-2-ylmethyl)-N-(2-phenylethyl) amine were prepared by general methods reported earlier [28].

Preparation of 1

N-(pyrrol-2-ylmethyl)-N-butylamine, (2.0 mmol) in ethanol was mixed with carbon disulfide (2.0 mmol) under ice cold condition. To the resultant yellow dithiocarbamic acid solution, aqueous solution of $HgCl_2$ (1.0 mmol) was added with constant stirring. The solid which precipitated was washed several times with cold water and then dried (**scheme-2**). Yield: 80%, mp: 126°C. IR (KBr, cm^{-1}): ν = 3389 (ν_{N-H}), 1494 (ν_{C-N}), 1028 (ν_{C-S}): ^{1}H NMR (400 MHz, $CDCl_3$): δ 0.95 (6H, N-CH_2-CH_2-CH_2-C**H**$_3$); 1.36 (m, N-CH_2-CH_2C**H**$_2$-CH_3); 1.70 (m, N-CH_2-

C**H**$_2$-CH$_2$-CH$_3$); 3.67 (t, 4H, N-C**H**$_2$-CH$_2$-CH$_2$-CH$_3$); 4.94 (s, 4H, N-C**H**$_2$ (pyrrole)); 6.10-6.13 (4H, H-3 and H-4(pyrrole)); 6.80 (d, 2H, H-5(pyrrole)); 9.32 (2H, N**H**-pyrrole): ^{13}C NMR (100 MHz, $CDCl_3$): δ 13.7 (N-CH$_2$-CH$_2$-CH$_2$-**C**H$_3$); 20.0 (N-CH$_2$-CH$_2$-**C**H$_2$-CH$_3$); 28.5 (N-CH$_2$-**C**H$_2$-CH$_2$-CH$_3$); 52.8 (N-**C**H$_2$-CH$_2$-CH$_2$-CH$_3$); 56.2 (N-**C**H$_2$(pyrrole)); 107.8, 109.3, 119.1, 125.7 (pyrrole ring carbons); 203.6 (N**C**S$_2$): Anal. Calcd. for $C_{20}H_{30}HgN_4S_4$ (%): C, 36.66; H, 4.61; N, 8.55; found (%): C, 36.51; H, 4.57; N, 8.48.

Preparation of 2

A method similar to that described for the synthesis of **1** was adopted; however, N-(pyrrol-2-ylmethyl)-N-(2-phenylethyl)amine was used instead of N-(pyrrol-2-ylmethyl)-N-butylamine (Scheme **2**). Yield: 79%, mp: 130°C, IR (KBr, cm^{-1}): ν = 3405 (ν_{N-H}), 1481 (ν_{C-N}), 1029 (ν_{C-S}): ^{1}H NMR (400 MHz, $CDCl_3$): δ 3.03 (t, 4H, CH$_2$-C**H**$_2$-C$_6$H$_5$); 3.89 (t, 4H, C**H**$_2$-CH$_2$-C$_6$H$_5$); 4.83 (s, 4H, C**H**$_2$-(pyrrole)); 6.12-613 (4H, H-3 and H-4(pyrrole)); 6.80 (d,2H, H-5(pyrrole)); 7.21-7.31(phenyl ring protons); 9.19 (2H, NH-pyrrole): ^{13}C NMR (100 MHz, $CDCl_3$): δ 32.9 (N-CH$_2$-**C**H$_2$-C$_6$H$_5$); 54.0 (**C**H$_2$-CH$_2$-C$_6$H$_5$); 57.7 (C**H**$_2$-pyrrole); 108.0, 109.5, 119.3, 125.5,126.9, 128.8, 137.8 (aromatic ring carbons); 204.1 (N**C**S$_2$) Anal. Calcd. for : $C_{28}H_{30}HgN_4S_4$ (%):C, 44.76; H, 4.02; N, 7.46; found (%): C,44.57; H, 4.03; N, 7.93.

2.4.2. Preparation of mercury sulfides

0.5 g of **1** was mixed with 15 ml triethylenetetraamine in a round bottom flask and then the content of the flask was refluxed for 15 minutes. The dark red color precipitate was filtered off and washed with methanol several times to remove the excess triethylenetetramine .

Similar procedure was adopted to prepare mercury sulfide from complex **2**.

3. Result and discussion

3.1. Spectroscopic characterization

IR spectra of **1** and **2** are shown in Figures **S1** and **S2**. Characteristic dithiocarbamate vibrations for complexes **1** and **2** are found at 1494 and 1481cm^{-1} ($\nu_{C\text{-}N}$ (thioureide)) and 1028 and 1029 cm^{-1} ($\nu_{C\text{-}S}$), respectively. The presence of only one band in the region 1000 ±50 cm^{-1} supports the bidentate coordination of dithiocarbamate ligand, while the thioureide band near 1490 cm^{-1} indicates considerable double-bond character in the C–N bond. This behavior may be attributed to the electron- releasing ability of amines, which forces high electron density towards the sulfur atoms via the thioureide π-system, thus producing double bond character and the $\nu_{C\text{-}N}$ vibration is observed between single ($\nu_{C\text{-}N}$ = 1350-1250 cm^{-1}) and double ($\nu_{C\text{-}N}$ = 1690-1640 cm^{-1}) bond energies.

^{1}H NMR and ^{13}C NMR spectra of **1** and **2** are given in Figures **S3-S6**. ^{1}H and ^{13}C NMR spectra of both the complexes are typical of diamagnetic species and are consistent with their chemical compositions. The ^{1}H NMR spectra of both complexes **1** and **2** reveal the NH proton signal at 9.32 and 9.19 ppm, respectively. This indicates that there is no direct metal ion coordination to the deprotonated pyrrole nitrogen atoms. A typical singlet is found at 4.94 and 4.83 ppm for **1** and **2**, respectively due to the methylene protons attached to pyrrole ring. The characteristic resonances of the butyl and ethyl group of phenylethyl found in the aliphatic region also support the proposed formulae of the dithocarbamate derivates. Aromatic proton signals due to pyrrole and phenyl rings are appeared in the region 6.12-7.31 ppm.

In the ^{13}C NMR spectra of **1** and **2**, the $^{13}NCS_2$ carbon signals are appeared at 203.6 and 204.1 ppm. An upfield shift was observed for both the complexes compared to the NCS_2

chemical shift of bis (N-(pyrrol-2-ylmethyl)-N-butyldithiocarbamato-S,S′)nickel(II) (206.3 ppm) and bis(N-(pyrrol-2-ylmethyl)-N-(2-phenylethyl)dithiocarbamato-S,S′)nickel(II) (206.9 ppm) [28]. In general, the extent of deshielding is greater for the thioureide $N^{13}CS_2$ signal in main group metal dithiocarbamates than those of normal valence state transition metal dithiocarbamates [29]. Pyrrole and phenyl ring carbons are observed in the region 107.8-137.8 ppm.

3.2.Structural analysis of 1

The molecular structure of **1** is shown in **Fig 1** and selected bond lengths and angles are collected in **Table 2**. Single crystal X-ray structure indicates that complex **1** is a monomer. The Hg(II) centre is coordinated by two anisobidentate dithiocarbamate ligands that define S_4 coordination geometry. Two of the Hg–S bond distances, *i.e.* 2.4957(10) and 2.4771(10) Å are significantly shorter than the Hg–S bond distances, *i.e.* 2.6327(11) and 2.6472(10) Å. There is a large compression of the dithiocarbamate bite angles S1–Hg–S2 (71.10(3)°) and S3–Hg–S4 (71.02(3)°). These acute chelate angles introduce significant distortions in the coordination geometry. These lead to enlargement of the other S–Hg–S angles with respect to the ideal tetrahedral angle (109.5°). The configuration around the mercury atom is a strongly distorted tetrahedral. The distorted tetrahedral coordination geometry (motif I) has been observed previously in the structure of mercury(II) dithiocarbamates [30]. The four membered chelate rings containing atoms Hg–S2–C10–S1 and Hg–S3–C20–S4 are coplanar within experimental error. S4 sulfur atom forms intermolecular hydrogen bond with pyrrole NH proton H1 (**Fig 2**). Two intermolecular C–H···π interactions between H5A and gravity centre of pyrrole ring [(C16-C19,N4)], H14A and cg[(C6-C9,N4)] result in a dimer (**Fig 3).** There are also four

intramoleclular C-H···S interactions with distances in the range 2.516-2.724 Å (**Fig. S7 and Table-3**).

3.3. Structural analysis of 2

Selected bond lengths and angles are listed in **Table 4**. Asymmetric unit of **2** is shown in **Fig 4a**. Two dithiocarbamate ligands in bis(N-(pyrrol-2-ylmethyl)-N-(2-phenylethyl) dithiocarbamato-S,S′)mercury(II) (**2**) are tridentate. In the asymmetric unit, Hg1 is coordinated by S2 and S3. The S1 and S4 coordinated to $Hg1^{i}$ and $Hg1^{ii}$, respectively. S2 and S4 are also coordinated to $Hg1^{i}$ and $Hg1^{ii}$, respectively (**Fig. 4b**). In the chain structure, each mercury atom is coordinated to six sulfur atoms (S2, S3, $S1^{i}$, $S2^{i}$, $S3^{ii}$, $S4^{ii}$) at distances of 2.501-2.939 Å . The geometry of the coordination polyhedron [HgS6] is distorted octahedral geometry with a range of angles from 66.02(4)°, *i.e.* the chelate angle to 163.38(4)° for S2–Hg1–$S3^{ii}$. The dithiocarbamate ligands are coordinated to mercury atoms, forming two extended eight-membered tricyclic moieties, [Hg1, $Hg1^{i}$, S1, S2, C1, $S1^{i}$, $S2^{i}$ and $C1^{i}$] and [Hg1, $Hg1^{ii}$,S3, S4, C15, $S3^{ii}$, $S4^{ii}$ and $C15^{ii}$], whose geometry can be approximated by chair conformations. These two moieties extended to form chain structure. There are four intramolecular C–H···S interactions observed (**Fig S8** and **Table 5).**

This structure is unique because of the following reasons: (i) This is the first example of octahedral mercury(II) dithiocarbamate complex whereas the central metal atom in zinc trial dithiocarbamate complexes is usually four or five coordinated [6]. (ii) In this complex, both dithiocarbamate ligands are triconnective and bridging. (iii) The chain structure is different from known structural motifs I–VI (see introduction).

In both complexes, Hg–S distances are asymmetric. However, C–S distances are symmetric and are shorter than the C–S single bond distance (1.81Å). Therefore all the C–S bonds in both the structures are of partial double bond character as observed in most of the dithiocarbamates [31]. The short thioureide C–N distances [1.330 (5) and 1.331(6) for **1** and **2**, respectively] in both the complexes indicate bonds have these double that these bonds have strong double bond character and that the π-electron density is delocalized over the S_2CN moiety.

Single crystal X-ray structural analysis of **1** and **2** show that complexes **1** and **2** adopt monomeric and polymeric chain structures, respectively. In complex **1**, both dithiocarbamate ligands function as anisobidentate and coordinated to the same mercury atom. The coordination geometry around Hg atoms is distorted tetrahedral. In complex **2**, both dithiocarbamate ligands act as tridentate and coordinated to three mercury atoms. The geometry of the coordination polyhedron is distorted octahedral. The structural difference between **1** and **2** are due to the size and electronic effects of the N-bound organic moiety of the dithiocarbamate ligands and also crystal packing effects.

3.4 Optimized structure

To compare the optimized structures and energy gap (HOMO ~ LUMO) of complexes **1** and **2** and to investigate reactive sites in **1** and **2**, we tried to do DFT calculations for **1** and **2**. But we could not obtain the DFT calculation results for the chain structure of **2**. Therefore, herein we report the theoretical studies for **1**. Selected bond distances and angles for **1** obtained by X-ray diffraction analysis and also calculated by DFT are given in **Table 6.** In the optimized structure, (Fig. S9) N-(pyrrol-2-ylmethyl)-N-butyldithiocarbamate ligand acts as bidentate. Two ligands

coordinate to mercury centre forming a tetrahedral geometry, similar to the structure obtained from the single crystal X-ray structure determination. Comparison of bond lengths and angles indicates a slight difference except S4–Hg–S1 angle. The observed slight differences could be attributed to the fact that the geometric parameters from the DFT calculations were generated in gaseous phase, while the experimental X-ray data were obtained in solid state. The large difference between calculated and experimental S4–Hg–S1 angle (20.438 °) may be due to the intermolecular interaction of S4···H1observed in solid state. This interaction is absent in optimized structure.

3.5 Frontier molecular orbitals

The two states of molecular orbitals, HOMO and LUMO give further understanding of the electronic state and reactivity of molecules. **Fig 5** exhibits the HOMO and LUMO of the molecule. The mercury predominantly contributes to the HOMO, while the remaining are from the four S atoms of the ligand. LUMO mainly located on pyrrole ring and a small contributions from S, N of NCS2 moiety to LUMO. The HOMO (-2.0889 eV) and LUMO (-5.8958 eV) is separated by an energy gap of 3.8070 eV. This gap is related to the stability and reactivity of the complex.

3.6 Molecular electrostatic potential (MEP) surfaces

To investigate reactive sites for nucleophilic and electrophilic attack, the MEP surfaces were plotted by DFT calculations. The plot of MEP surface of **1** is shown in **Fig. S10**.Different values of electrostatic potential at the surfaces are represented by different colours. The electrostatic potential increases in the order: red (most negative electrostatic potential) < orange < yellow < green < blue (most positive electrostatic potential) [32,33]. The negative electrostatic

potential regions of the MEP surfaces are related to electrophilic reactivity and the positive electrostatic potential regions to nucleophilic reactivity [34,35]. The most negative region of the MEP surfaces is mainly localized over S atoms of NCS_2 group and N atom of pyrrole indicating that they are the most suitable atomic sites for elelctrophilic attack. The positive region is localized on N atom of NCS_2 group exhibiting that it is possible site for attack by nucleophiles.

3.7 Characterization of metal sulfide nanoparticles

Mercury sulfide nanoparticles from complexes **1** and **2** are represented as samples **1** and **2**, respectively. Powder X-ray diffraction patterns of the samples **1** and **2** displayed in **Fig 6**. All the diffractions peaks in powder X-ray diffraction patterns of samples **1** and **2** could be indexed to be hexagonal phase (α-HgS, cinnabar) and cubic phase (β-HgS, meta cinnabar). These are in good agreement with standard data from the JCPDS card No. 89-7103 and 89-0432 for sample **1** and **2**, respectively. In both the cases, no peaks due to any impurities were detected, revealing the presence of single phase in the product.

TEM images of samples **1** and **2** are shown in **Fig 7**. TEM images of sample **1 (Fig.7(a)** and **(b)**) reveal that most of the particles are spherical with diameter in the range 14-36 nm. A few hexagonal and cubic particles are also present in the sample **1**. In the case of sample **2**, all the particles are spherical with diameter in the range 20-30nm.

Powder X-ray diffraction and TEM studies support that the different phases, shape and size of HgS nanoparticles can be prepared using mercury(II) dithiocarbamate complexes containing various N-bound organic moiety of dithiocarbamate .

Energy dispersive X-ray spectra (**Fig 8**) of both the samples exhibit strong signals for mercury and sulfur. This confirms that the solvothermal decomposition of both the complexes **1** and **2** yield mercury sulfide. Elemental analytical data obtained from EDS of sample **1** reveal that the atomic percentage of Hg and S are 43.68 and 56.32 (ratio: 1:1.29), respectively. This reveals that a higher number of sulfur atoms present in the products compared to mercury. This may be due to the presence of some vacant sites of Hg^{2+} or sulfur dangling bonds in the sample **1**. In the case sample of **2**, the atomic percentage of mercury and sulfur [53.15:46.85; ratio: 1:0.88] indicate the presence of excess Hg^{2+} in the sample **2.**

UV-vis absorption spectra of sample **1** and **2** are displayed in **Fig 9(a) and (b)**, respectively. An absorption maxima is appeared at 220 nm in the UV-Vis absorption spectra of both the samples. A blue shift is observed in the absorption maxima relative to the bulk HgS (620 nm) [36]. Generally, the absorption maxima (λ_{max}) decreases with a decreasing size of the nanoparticles as a consequences of quantum confinement of the photogenerated electron-hole carriers [37].

Photoluminescence spectra of samples **1** and **2** are shown in **Fig 10(a) and (b),** respectively. The spectra of samples **1** and **2** exhibit a broad emission peak at 364 and 340 nm, respectively on excitation at 265 and 270 nm, respectively. These peaks are due to the core state radioactive decay from CB to VB and the blue shift of the emission peak compared to those of bulk HgS (588 nm) [38] is attributed to the quantum confinement effect.

Fig 11 shows the FTIR spectra of samples **1** and **2**. In the spectra of both samples, a broad band around 3400 cm^{-1} for samples **1** and **2** correspond to the stretching vibration of N–H and the peaks in the region 2851-2959 cm^{-1} are assigned to the stretching vibrations of aliphatic

C–H. No peaks observed due to the stretching vibrations of C–N (thioureide), C–S and aromatic C–H indicate the absence of dithiocarbamate ligands in the samples **1** and **2**.

4. Conclusions

In this contribution, two Hg(II) dithiocarbamate complexes were prepared and fully characterized. Crystal structure of **1** and **2** reveal that the complexes **1** and **2** are monomer and polymer respectively, and the geometries around each mercury atom in **1** and **2** are distorted tetrahedral and octahedral, respectively. This study suggests that the different structural motifs can be obtained by changing the N-bound organic moiety of the dithiocarbamate ligands. Three different morphological α-HgS and spherical β-HgS nanoparticles were obtained from **1** and **2,** respectively. This study also shows that various morphological and phase (α and β) HgS nanoparticles can be prepared from different mercury (II) dithiocarbamate complexes.

5. Supplementary data

CCDC 1488853 and 1488854 contain the supplementary crystallographic data for complexes **1** and **2**. This data can be obtained free of charge *via* http://www.ccdc.cam.ac.uk/conts/retrieving.html, or from the Cambridge Crystallographic Data Centre, 12 Union Road, Cambridge CB2 1EZ, UK; fax: (+44) 1223-336-033; or e-mail: deposit@ccdc.cam.ac.uk.

Acknowledgements

Dr. S. Thirumaran is thankful to University Grants Commission (UGC), India (F. No. 42-341/2013 (SR)) for providing fund for this research study. We are thankful to SAIF, Panjab University, Chandigarh, India, for recording TEM images.

Reference

[1] P.J. Heard, Prog Inorg Chem. 53 (2005) 1.

[2] G. Hogarth, Prog Inorg Chem. 53 (2005) 71.

[3] Z. Rehman, N. Muhammad, S. Ali, I.S. Butler, A. Meetsma, Inorg. Chim. Acta (2011) 381-388.

[4] P. Jamuna Rani, S. Thirumaran, Eur. J. Med. Chem. 62 (2013) 139.

[5] K.G. Mallikanjuuni, Eur. J. Chem. 2 (2005) 58.

[6] M. J. Cox, E.R.T.Tiekink, Inorg.Chem.Rev., 17 (1997) 1-23.

[7] E.R.T.Tiekink, Cryst Eng Comm 5 (2003) 101.

[8] D. C. Onwudiwe and P.A. Ajibade, J Chem Crystallogr. 41 (2011) 980-985.

[9] R. O. Howie, E.R.T. Tiekink, J. L. Wardell, S. M. S. V. Wardell, J. Chem Crystallogr. 39 (2009) 293-298.

[10] M. J. Cox and E. R. T. Tiekink, Z. Kristallogr., 214 (1999) 571.

[11]] G.Gomathi, S. Hussain Dar, S. Thirumaran, S. Ciattini, S. Selvanayagam, C.R. Chimie. 18 (2015) 499-510.

[12] N. Srinivasan, S. Thirumaran and S. Ciattini, RSC Adv., 4 (2014) 22971.

[13] D.C. Onwudiwe and P. A. Ajibade, Int. J. Mol. Sci., 12 (2011) 5538-5551.

[14] G. Gomathi, S. Thirumaran, S. Ciattini, Polyhedron. 102 (2015) 424-433.

[15] G. Marimuthu, K. Ramalingam, C. Rizzoli, M. Arivanandhan, J Nanopart Res 14 (2012) 710.

[16] D.C. Onwudiwe and P. A. Ajibade, Int. J. Mol. Sci., 13 (2012) 9502-9513.

[17] N. L. Pickette, P. O' Brien, Chem Rec. **1** (2001) 467.

[18] N. Tokyo, J. Appl.Phys. 461 (1975) 4857.

[19] S.S. Kale, C. D. Lokhande, J. Mater. Chem.Phys. 59 (1999) 242.

[20] A. M. Fernandez, M.T.S. Nair, P.K. Nair, J. Mater. Manuf. Process. 8 (1993) 535

[21] C.O. Monteriro, T. Trindade, J.H. Park, P.O. Brien, Chem. Vapour Depos. 6 (2000) 286.

[22] S.T. Lakshmikumar, A.C. Rastogi, Sol Energy Mater Sol Cells. 32 (1994) 7–19.

[23] P . Alivisatos, Nat Biotechnol 22 (2004) 47–52.

[24] G.G. Roberts, E. L. Lind, E. A. Davis, 30 (1969) 833-844.

[25] G.M. Sheldrick, SHELXS-97: Program for the Crystal Structure Refinement, University of Gottingen, Gottingen, Germany , 1997.

[26] G.M. Sheldrick, Acta Crystallogr. A 64 (2008) 112-122.

[27] M.J. Frisch, G.W. Trucks, H.B. Schlegel et at., Gaussion 03, Revision C.02, Pittisburg PA, (2003).

[28] E. Sathiyaraj, G. Gurumoorthy and S. Thirumaran. New.J.Chem. 39 (2015) 5336-5349.

[29] H.L.M. Gaal, J.W. Van Diesveld, F.W. Pijpers, J.G.M. Van Der Lindon. Inorg. Chem., 18 (1979) 3251

[30] M. Altaf, He. Stoeckli-evans, S. S. S. Batool, A. A. Isab, S. Ahmad, M. Saleem, S. Ahmad Awan and M. A. Shaheen , J Coord Chem. 63 (2010) 1176–1185.

[31] V. Venkatachalam, K. Ramalingam, U. Casellato and R. Graziani, Polyhedron. 16 (1997) 1211-1221.

[32] V.D. Vitnik, Z.J. Vitnik, N.R. Banjac, N.V. Valentic, G.S. Uscumlic, and I.O. Juranic,. Spectra Chim. Acta Part A 11**7** (2014) 42-53.

[33] M. Koparir, C. Orek, N.O. Alayunt, A.E. Parlak, P. Koparir, K. Sarac, S.D. Dastan and N. Cankaya, Commun. Comput. Chem, **1** (2013) 244-268.

[34] T.C. Zeyrek, J. Korean Chem Soc, **57** (2013) 461-471.

[35] M.V.S. Prasad, N.U. Sri, A. Veeraiah, V. Veeraiah, and K. Chaitanya, J. At. Mol. Sci, **4** (2013) 1-17

[36] A.K. Mahapatra, A.K. Dash, Phys. E. 35 (2006) 9.

[37] L. Brus, J. Phys. Chem. 90 (1986) 2555.

[38] A.R. Rao, V. Dutta, V.N. Singh, Adv. Mat. 20 (2008) 1945.

Table.1.Crystal data, data collection and refinement parameters for complexes 1 and 2

Parameters	**1**	**2**
Empirical formula	C_{20} H_{30} Hg N_4 S_4	C_{28} H_{30} Hg N_4 S_4
Formula weight	655.31	751.39
Crystal system	triclinic	monoclinic
Space group	P ī	P 2_1 /c
a/Å	8.3997(5)	8.5939(2)
b/Å	9.8463(5)	29.6100(7)
c/Å	15.2994(8)	11.0514(5)
α/º	103.904(4)	90
β/º	95.242(5)	91.928(3)
γ/º	93.949(5)	90
V/Å^3	1217.73(12)	2810.61(16)
Z	2	4
Dcalc/gcm^{-3}	1.685	1.613
μ/cm^{-1}	0.136	0.142
F(000)	644	1480
λ/Å	MoKα (0.71073)	MoKα (0.71073)
Index ranges	−11 ≤ h ≤ 11, −12 ≤ k ≤ 13, −20 ≤ l ≤ 20	−11 ≤ h ≤ 11, −27 ≤ k ≤ 37, −13 ≤ l ≤ 14
Reflections collected	5601	6481
Observed reflections [I > 2σ(I)]	4710	4902
Weighting scheme	w=1/[σ^2(F_o^2)+(0.0152P)^2+0.3842 P] where P=(F_o^2+2F_c^2) /3	w=1/ [σ^2 (F_o^2)+(0.0241P)^2] where P=(F_o^2+2F_c^2) / 3
Parameters refined	262	334
R[F^2 > 2σ(F^2)], wR(F^2)	0.0361, 0.0686	0.0452, 0.0847
GOOF	1.082	1.064

Table .2. Selected bond lengths (Å) and bond angles (°) of complex 1

Bond distances (Å)		Bond angles (°)	
Hg1 S3	2.4771(10)	S3 Hg1 S2	137.98(4)
Hg1 S2	2.4957(10)	S3 Hg1 S1	137.14(3)
Hg1 S1	2.6327(11)	S2 Hg1 S1	71.10(3)
Hg1 S4	2.6472(10)	S3 Hg1 S4	71.02(3)
S4 C20	1.720(4)	S2 Hg1 S4	132.62(3)
S3 C20	1.741(4)	S1 Hg1 S4	115.62(3)
S1 C10	1.728(4)	S1 C10 S2	118.5(2)
S2 C10	1.745(4)	C20 N3 C14	122.0(3)
N2 C10	1.330(5)	C20 N3 C15	122.8(3)
N4 C19	1.364(5)	S4 C20 S3	118.8(2)
N4 C16	1.372(5)	C14 N3 C15	115.2(3)
N3 C20	1.329(5)	C10 N2 C4	122.0(4)
N3 C14	1.481(5)	C10 N2 C5	122.2(3)
N3 C15	1.490(5)	N3 C20 S3	119.4(3)
N1 C9	1.361(5)	N2 C10 S1	121.8(3)
N1 C6	1.367(5	N2 C10 S2	119.8(3)
		N3 C20 S4	121.7(3)

Table.3. Geometric details of hydrogen bonding (Å,º) in 1

Interactions	**D–H**	**H···A**	**D···A**	**D–H···A**
C4 —H4A···S1[a]	0.97	2.619	3.026 (4)	105.47
C5—H5B···S2[a]	0.97	2.568	3.001 (4)	107.15
C15—H15B···S3[a]	0.97	2.516	3.007 (4)	111.32
C14—H14A···S4[a]	0.97	2.627	3.029 (4)	105.17
N1—H1···S4[b]	0.86	2.971	3.392 (4)	112.29
C14—H14A···Cg(C6-C9,N4)[c]	0.97	2.938	3.649	130.99
C5—H5A···Cg (C16-C19,N4)[c]	0.97	3.104	3.912	147.06

[a]-intramolecular C–H···S hydrogen bonding

[b]-Intermolecular N–H···S interactions

[c]-intermolecular C–H···π (chelate) interaction

Table .4. Selected bond lengths (Å) and bond angles (°) of complex 2

Bond distances (Å)			
Hg1 S1^{i}	2.5011(13)	S1 Hg1^{i} S3^{ii}	99.57(4)
Hg1 S4^{ii}	2.5016(13)	S4 Hg1^{ii} S3^{ii}	67.02(4)
Hg1 S2	2.7927(14)	S2 Hg1^{ii} S3	163.38(4)
Hg1 S3^{ii}	2.8747(14)	S1 Hg1 S3	99.80(4)
Hg1 S3	2.8823(15)	S4 Hg1^{i} S2^{i}	103.71(4)
Hg1 S2^{i}	2.9391(14)	S2 Hg1 S2	83.74(4)
S2 C1	1.726(5)	S3 Hg1^{i} S2	111.54(4)
S3 C15	1.716(5)	S3 Hg1 S2	161.83(4)
N3 C15	1.337(6)	C1 S2 Hg1	99.18(16)
N3 C16	1.469(5)	C1 S2 Hg1	79.97(18)
N3 C24	1.473(6)	Hg1 S2 Hg1	96.26(4)
N1 C1	1.325(6)	C15 S3 Hg1	80.60(18)
N1 C2	1.478(5)	C15 S3 Hg1	99.82(19)
N1 C10	1.478(6)	N1 C2 C3	112.5(4)
N4 C28	1.359(7)	N1 C2 H2A	109.1
		N1 C10 H10A	108.7
		N1 C10 H10B	108.7
Bond angles (°)		N1 C1 S2	120.5(4)
S1 Hg1^{i} S4^{ii}	159.76(5)	N1 C1 S1	119.7(4)
S1 Hg1^{i} S2	92.54(4)	S2 C1 S1	119.7(3)
S4 Hg1^{ii} S2	103.94(4)		

Symmetry code: *i* = 1-x, 2-y, -z;
ii= -x, 2-y, -z

Table.5. Geometric details of hydrogen bonding (Å,º) in 2

Interactions	**D–H**	**H···A**	**D···A**	**D–H···A**
C2 —H2A···S1[a]	0.97	2.574	3.014 (5)	107.73
C10—H10B···S2[a]	0.97	2.602	3.013 (5)	105.69
C24—H24A···S3[a]	0.97	2.536	2.983 (5)	108.04
C16—H16A···S4[a]	0.97	2.616	3.018 (5)	105.17

[a]-intramolecular C–H···S hydrogen bonding

Table. 6. Theoretical and experimental of selected bond distances(Å) and bond angles(˚) for complex 1

Bond distances (Å)	**XRD**	**DFT/LanL2DZ**
Hg1-S1	2.633(1)	2.7274
Hg1-S2	2.496(1)	2.7685
Hg1-S3	2.477(1)	2.7661
Hg1-S4	2.647(1)	2.7288
S1-C10	1.728(4)	1.7994
S2-C10	1.745(4)	1.8073
S3-C20	1.740(5)	1.8078
S4-C20	1.721(4)	1.7988
N2-C10	1.329(5)	1.3462
N3-C20	1.329(5)	1.3463
N2-C4	1.467(5)	1.4914
N2-C5	1.486(6)	1.5064
N3-C14	1.481(5)	1.4913
N3-C15	1.490(5)	1.5065
Bond angles (˚)	**XRD**	**DFT/LanL2DZ**
S4-Hg1-S3	71.02(3)	69.033
S4-Hg1-S1	115.62(3)	136.058
S4-Hg1-S2	132.62(3)	132.807
S3-Hg1-S1	137.14(3)	133.162
S3-Hg1-S2	137.97(4)	128.693
S1-Hg1-S2	71.10(3)	69.029
S1-C10-S2	118.4(2)	119.414
S1-C10-N2	121.8(3)	120.205
S2-C10-N2	119.8(3)	120.379
S4-C20-S3	118.8(2)	119.387
S4-C20-N3	121.7(3)	120.288
S3-C20-N3	119.5(3)	120.322
C10-N2-C5	122.2(3)	122.431
C10-N2-C4	122.0(3)	122.896
C5-N2-C4	115.8(3)	114.664
C15-N3-C14	115.2(3)	114.663
C15-N3-C20	122.7(3)	122.375
C14-N3-C20	122.0(3)	122.951

Schemes and Figure captions

Scheme 1. Structural variations in mercury(II) dithiocarbamates

Scheme 2. Preparation of complexes **1** and **2**.

Figure 1. ORTEP of complex **1**.

Figure 2. Intermolecular C-H···S interaction in complex **1**.

Figure 3. Intermolecular C–H···π (chelate) interaction in complex **1**.

Figure 4. (a) Asymmetric unit and (b) ORTEP of complex **2** (Symmetry code: *i* = 1-x, 2-y, -z; *ii*= -x, 2-y, -z)

Figure 5. Graphical images of the HOMO and LUMO of complex **1**

Figure 6. Powder X-ray diffraction patterns of (a) α-HgS and (b) β-HgS

Figure 7. TEM images of (a) α-HgS and) (b) β-HgS

Figure 8. Energy dispersive spectra of (a) α-HgS and (b) β-HgS

Figure 9. UV-Vis spectra of (a) α-HgS and (b) β-HgS.

Figure 10. PL spectra of (a) α-HgS and (b) β-HgS.

Figure 11. IR Spectra of (a) α-HgS and (b) β-HgS.

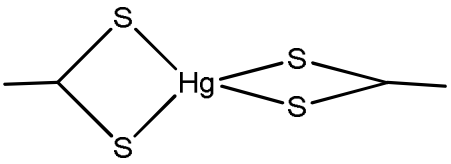

(I)

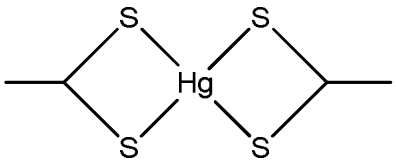

(II)

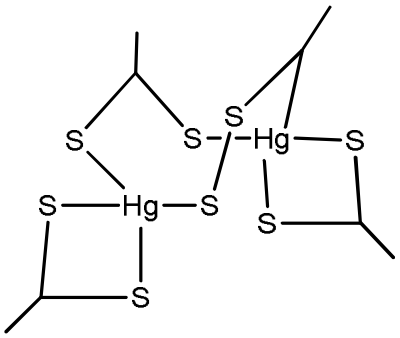

(III)

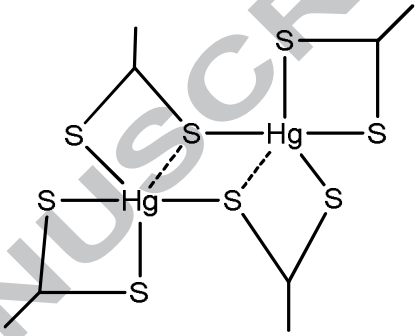

(IV)

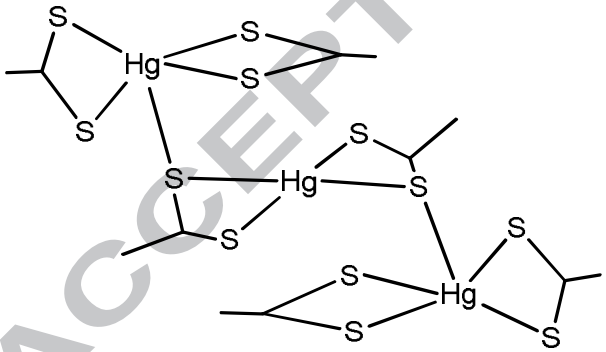

(V)

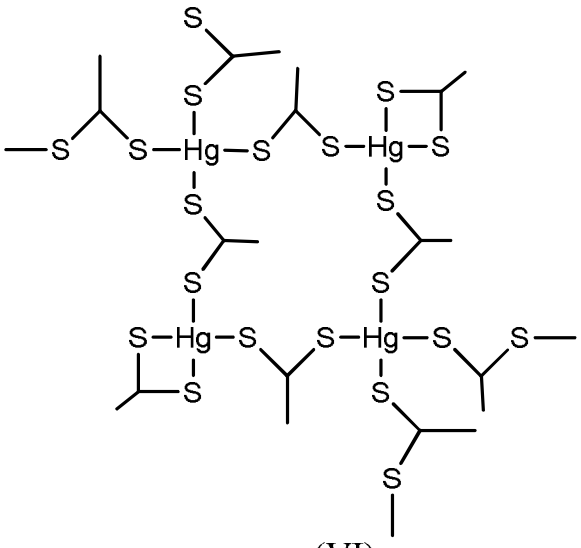

(VI)

Scheme-1

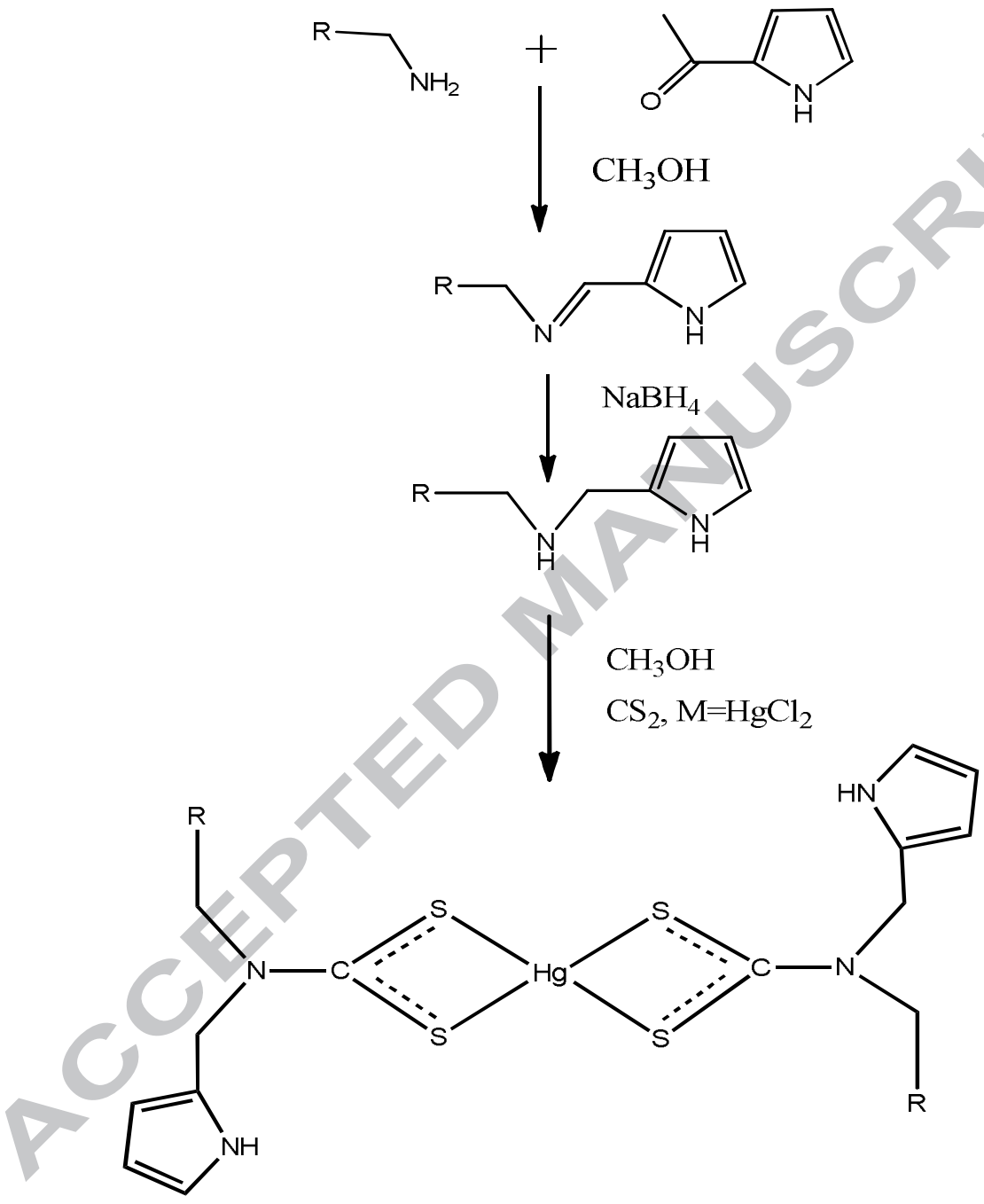

R= n-Butylamine, 2-Phenylethylamine

Scheme-2

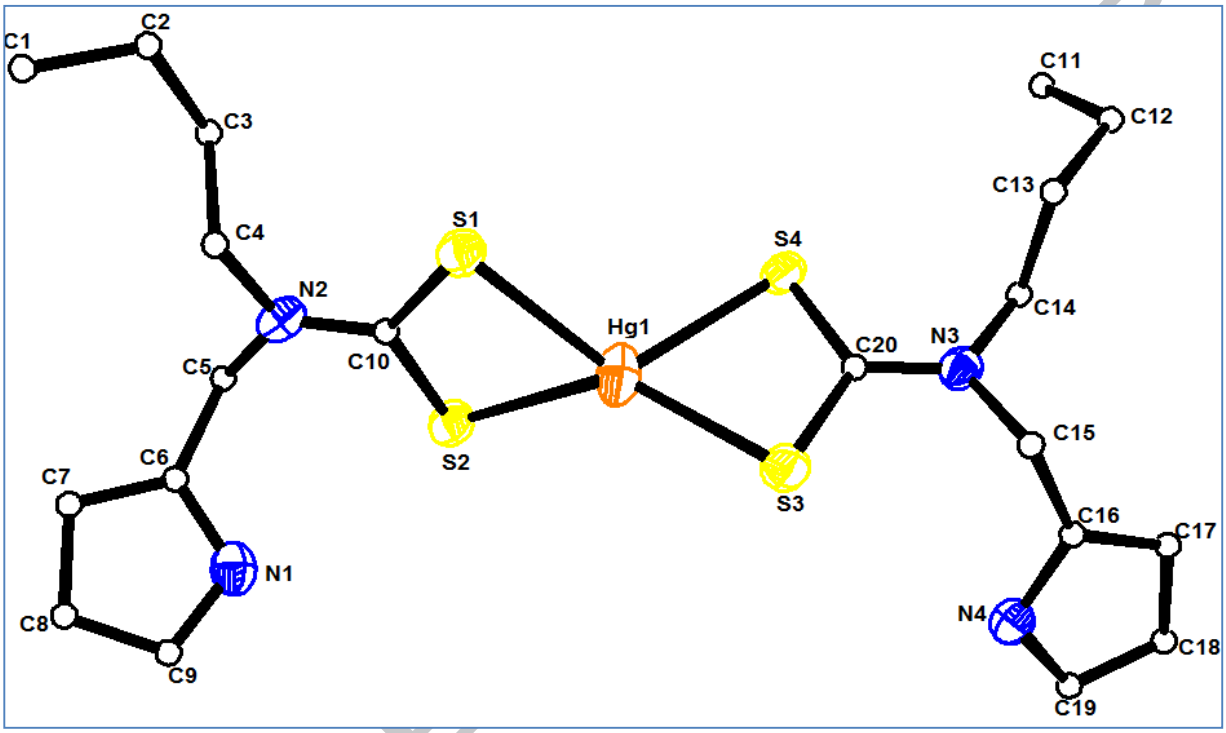

Figure 1.

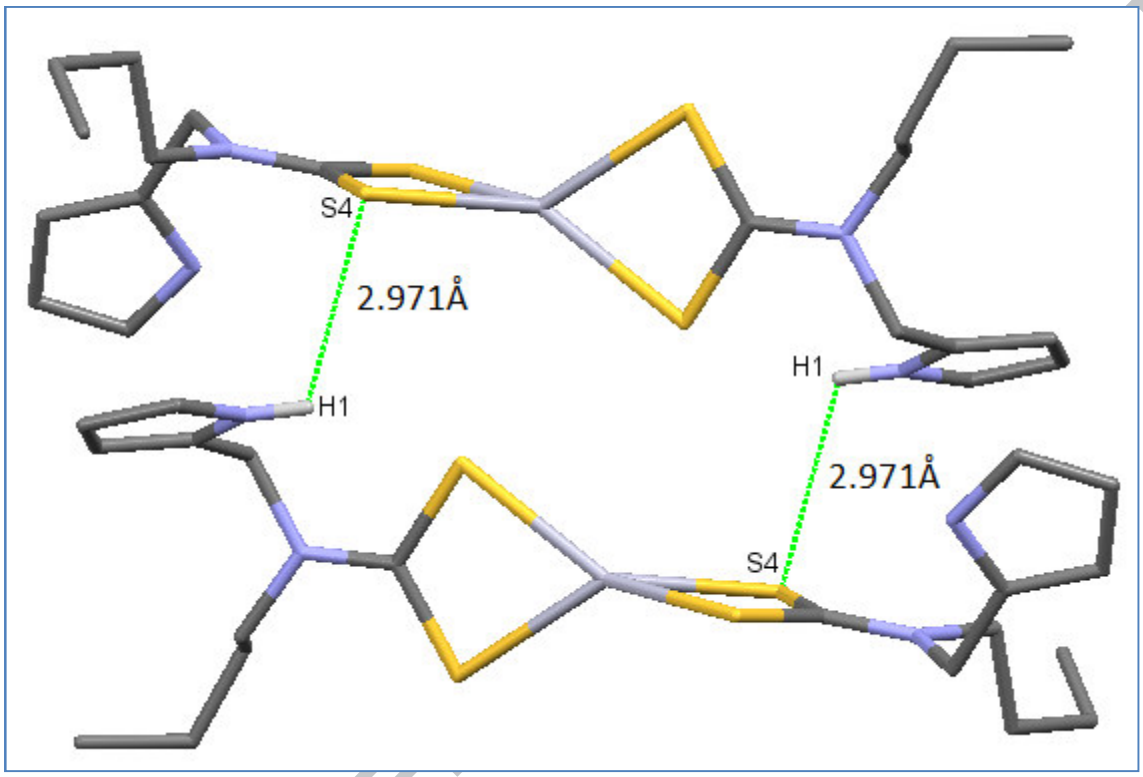

Figure 2.

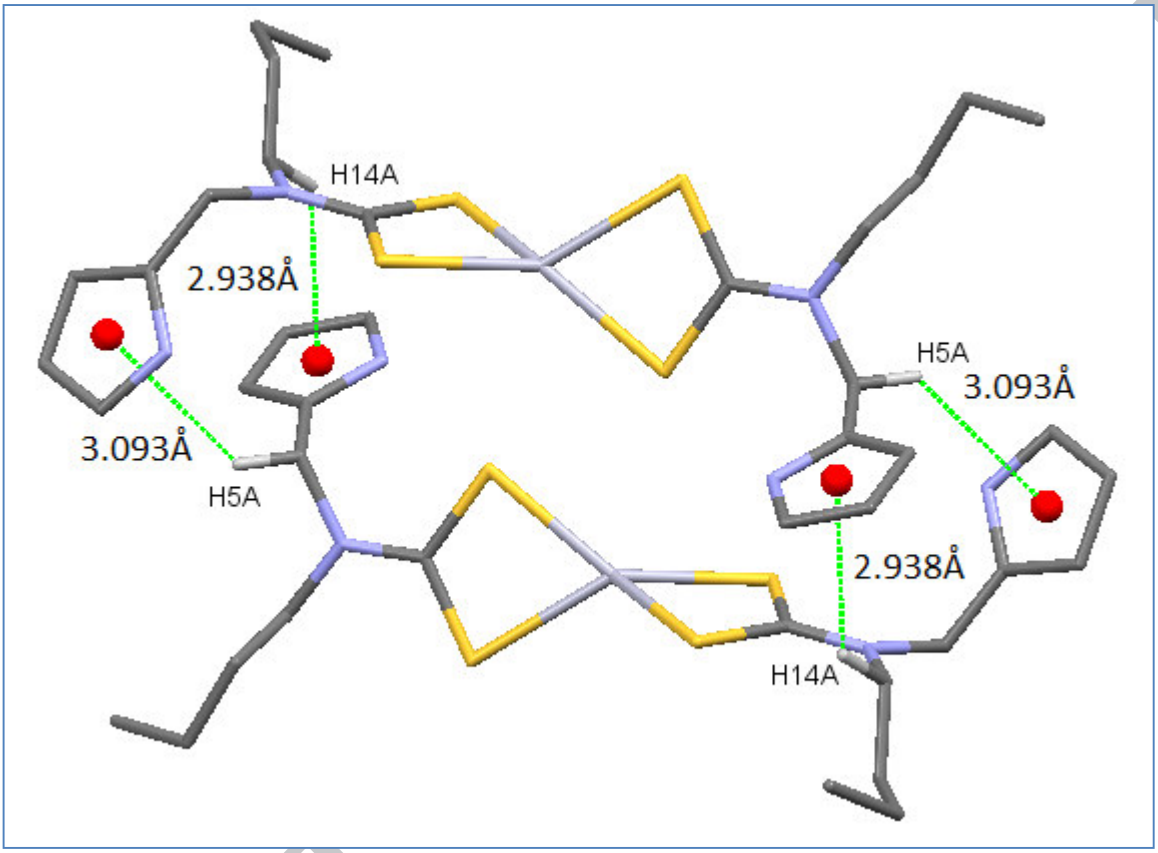

Figure 3.

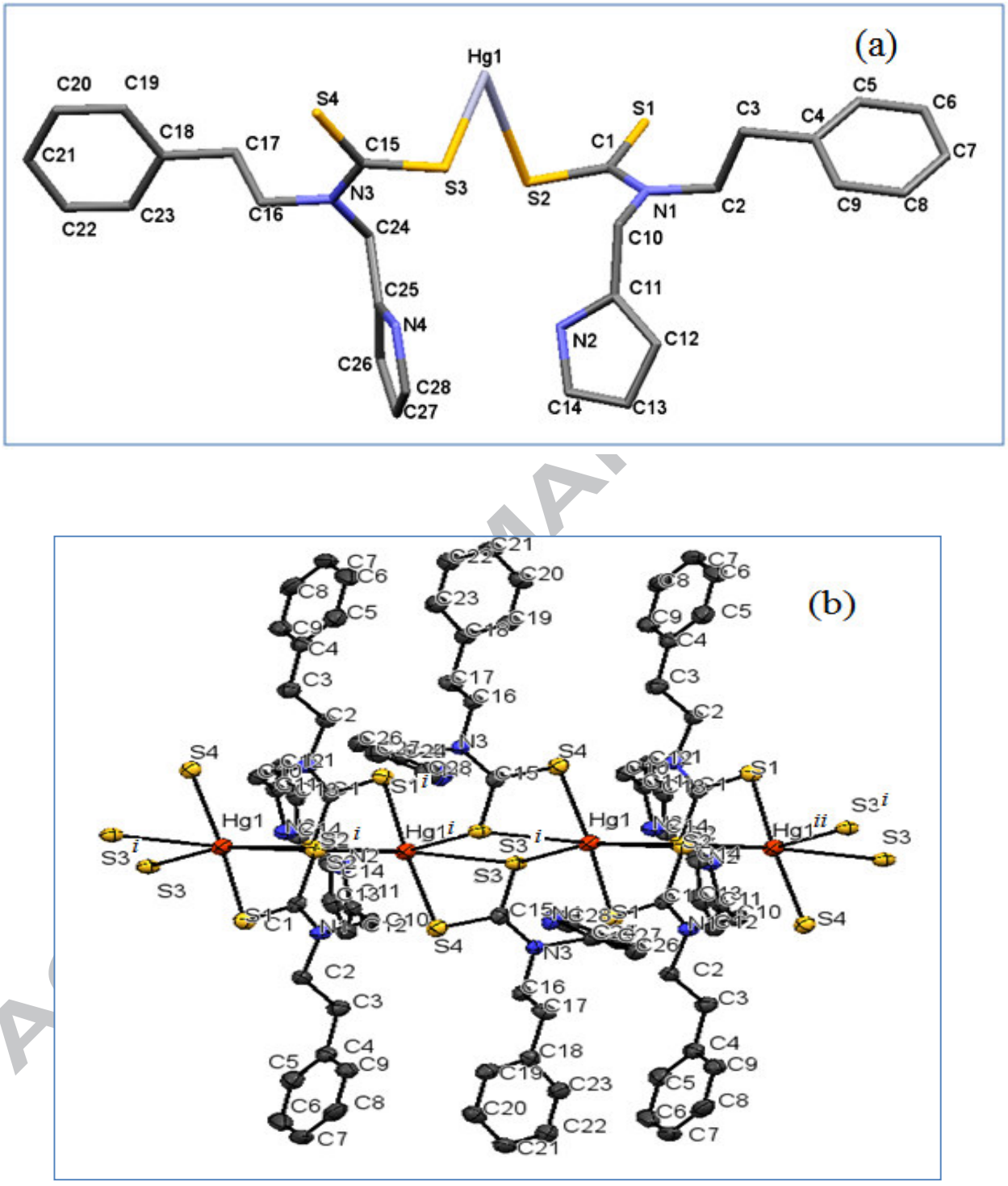
(a)
Hg1
S4
S1
C20
C19
C18
C17
C15
C1
C3
C4
C5
C6
C7
C21
S3
S2
C2
C9
C8
C22
C23
C16
N3
N1
C24
C10
C25
C11
N4
N2
C12
C26
C28
C27
C14
C13
(b)
Hg1
Hg1i
Hg1ii
S3
S4
S1
N3
N2
C15
C16
C17
C18
C19
C20
C21
C22
C23
C24
C25
C26
C27
C28
C1
C2
C3
C4
C5
C6
C7
C8
C9
C10
C11
C12
C13
C14

Figure 4.

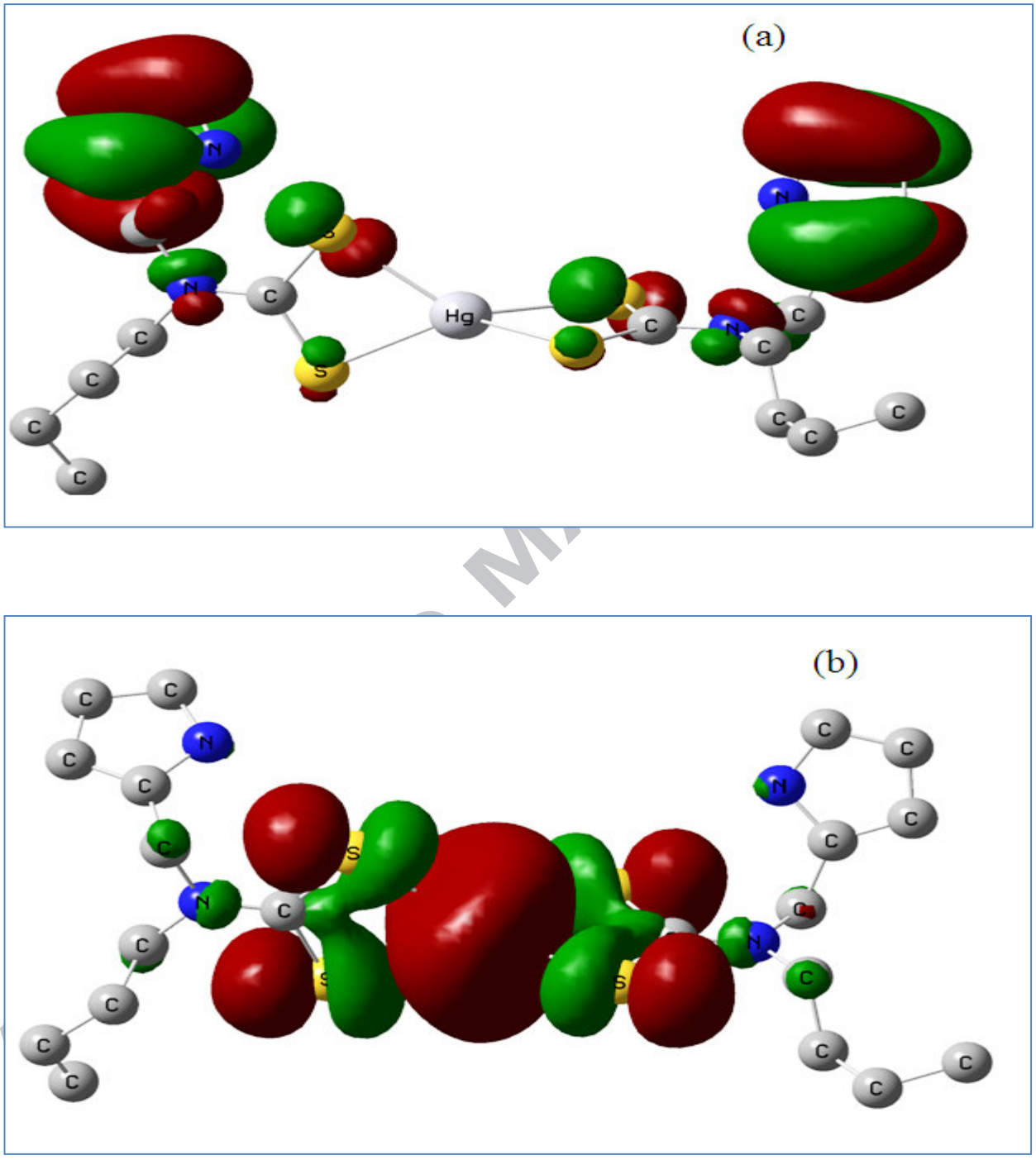

Figure 5.

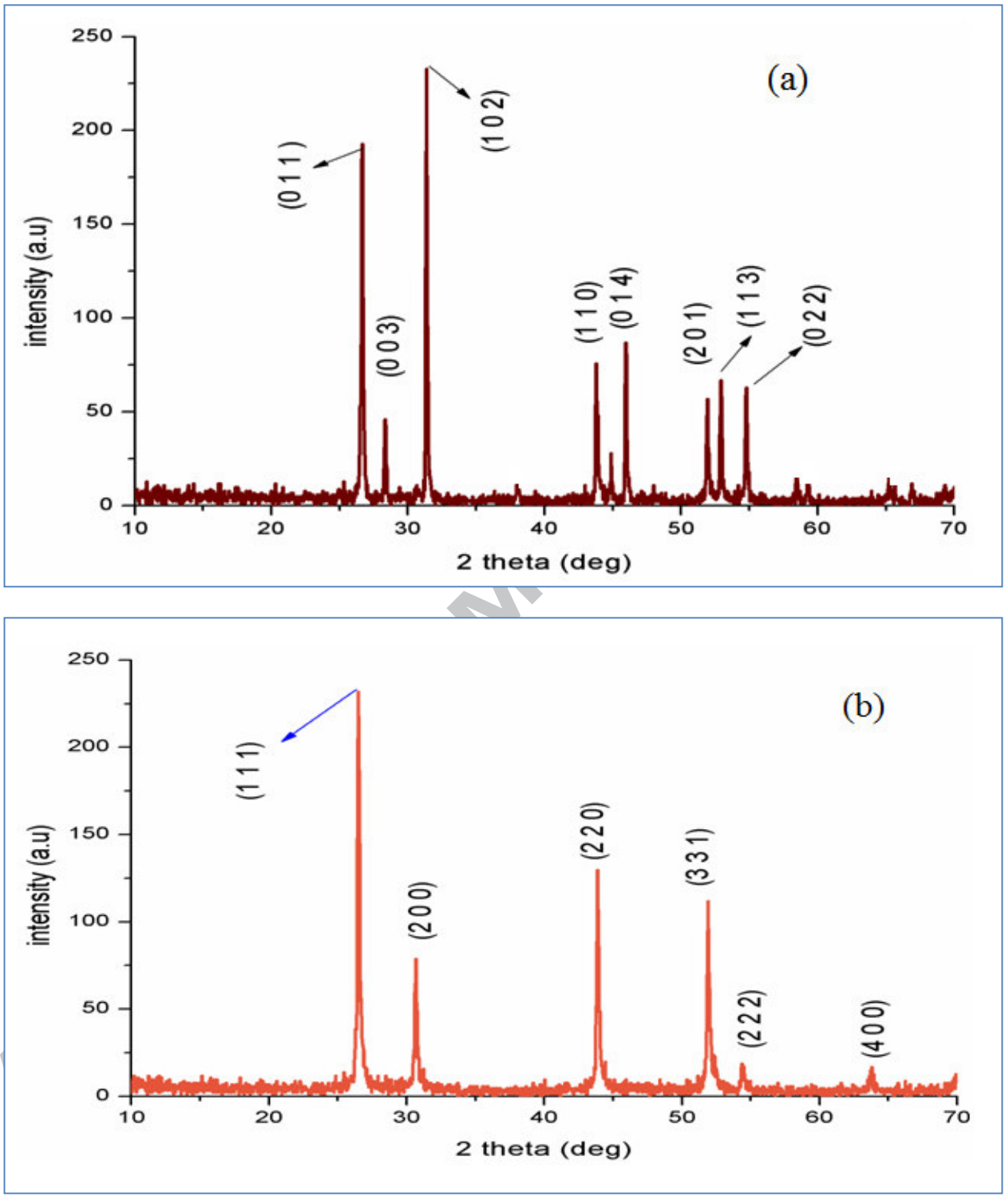
(a)
intensity (a.u)
2 theta (deg)
(0 1 1)
(0 0 3)
(1 0 2)
(1 1 0)
(0 1 4)
(2 0 1)
(1 1 3)
(0 2 2)
(b)
intensity (a.u)
2 theta (deg)
(1 1 1)
(2 0 0)
(2 2 0)
(3 3 1)
(2 2 2)
(4 0 0)

Figure 6.

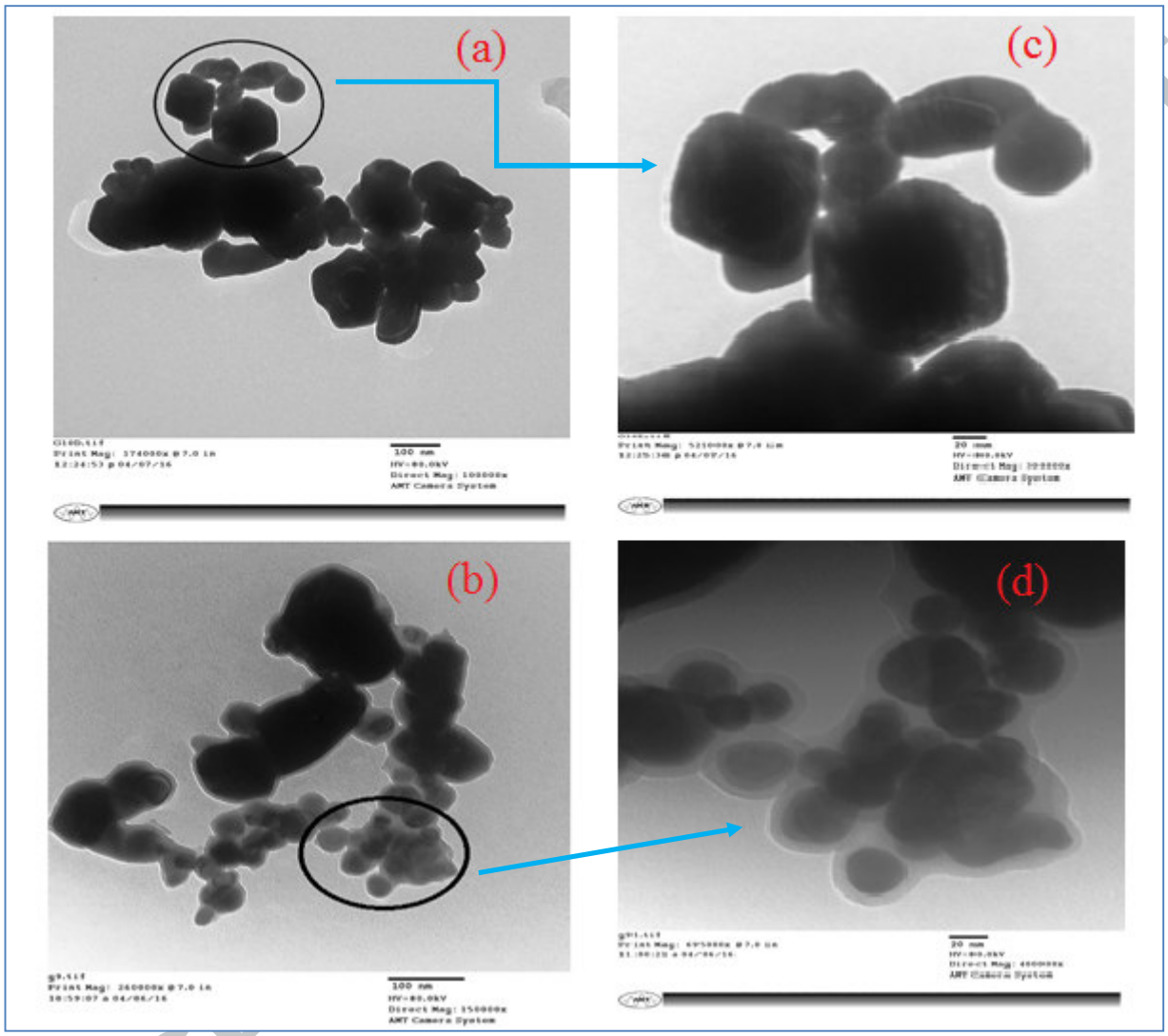

Figure 7.

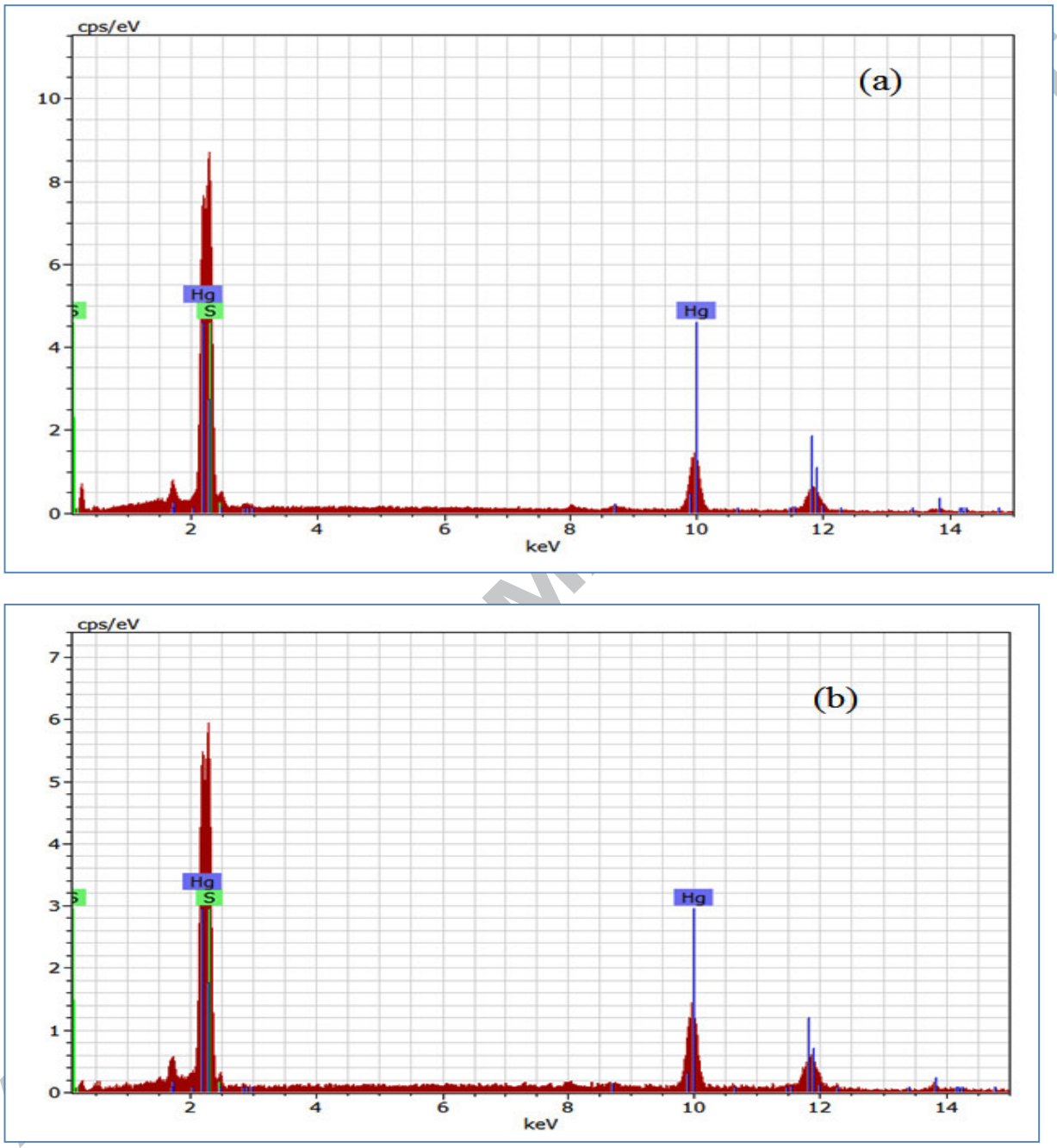

Figure 8.

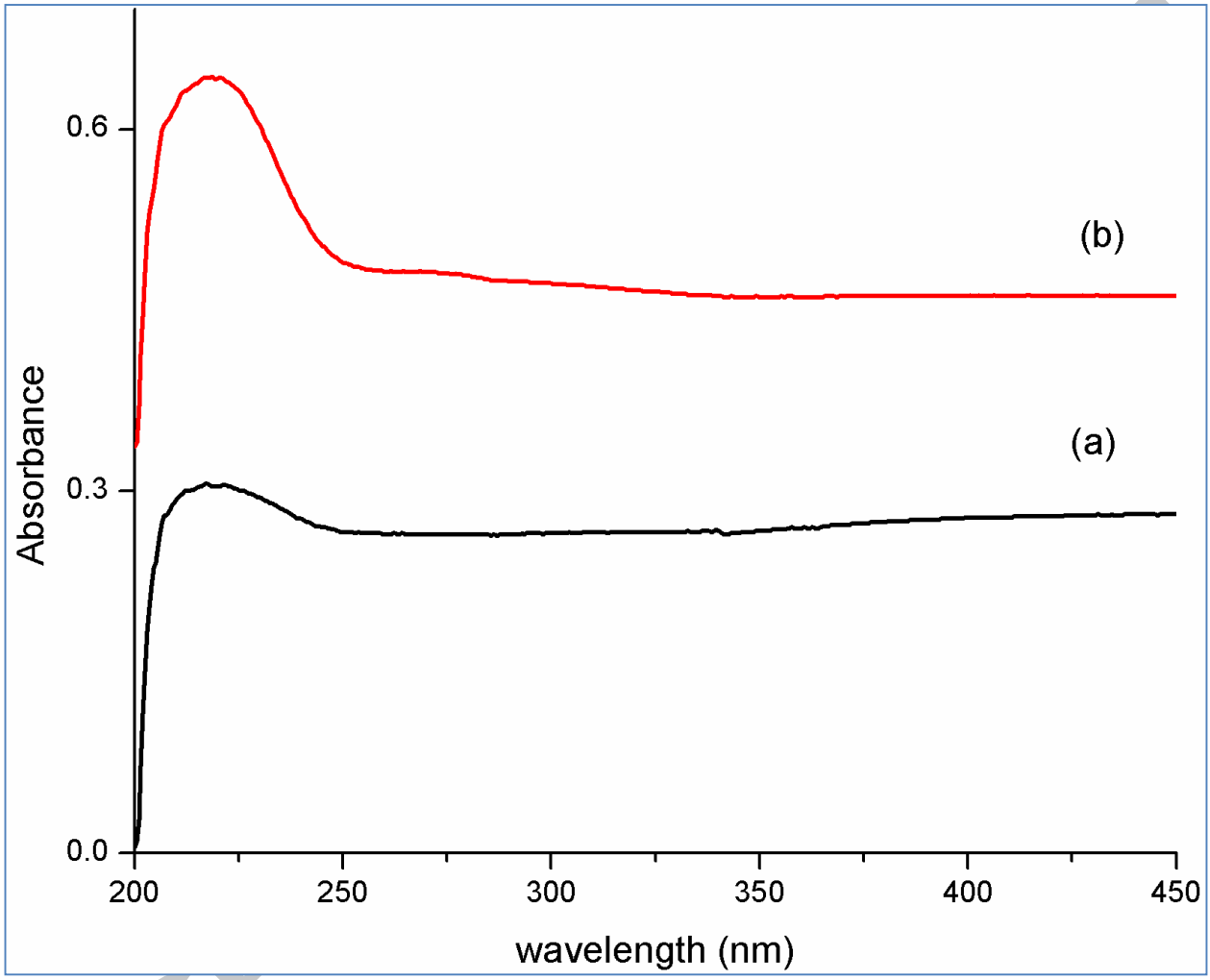

Figure 9.

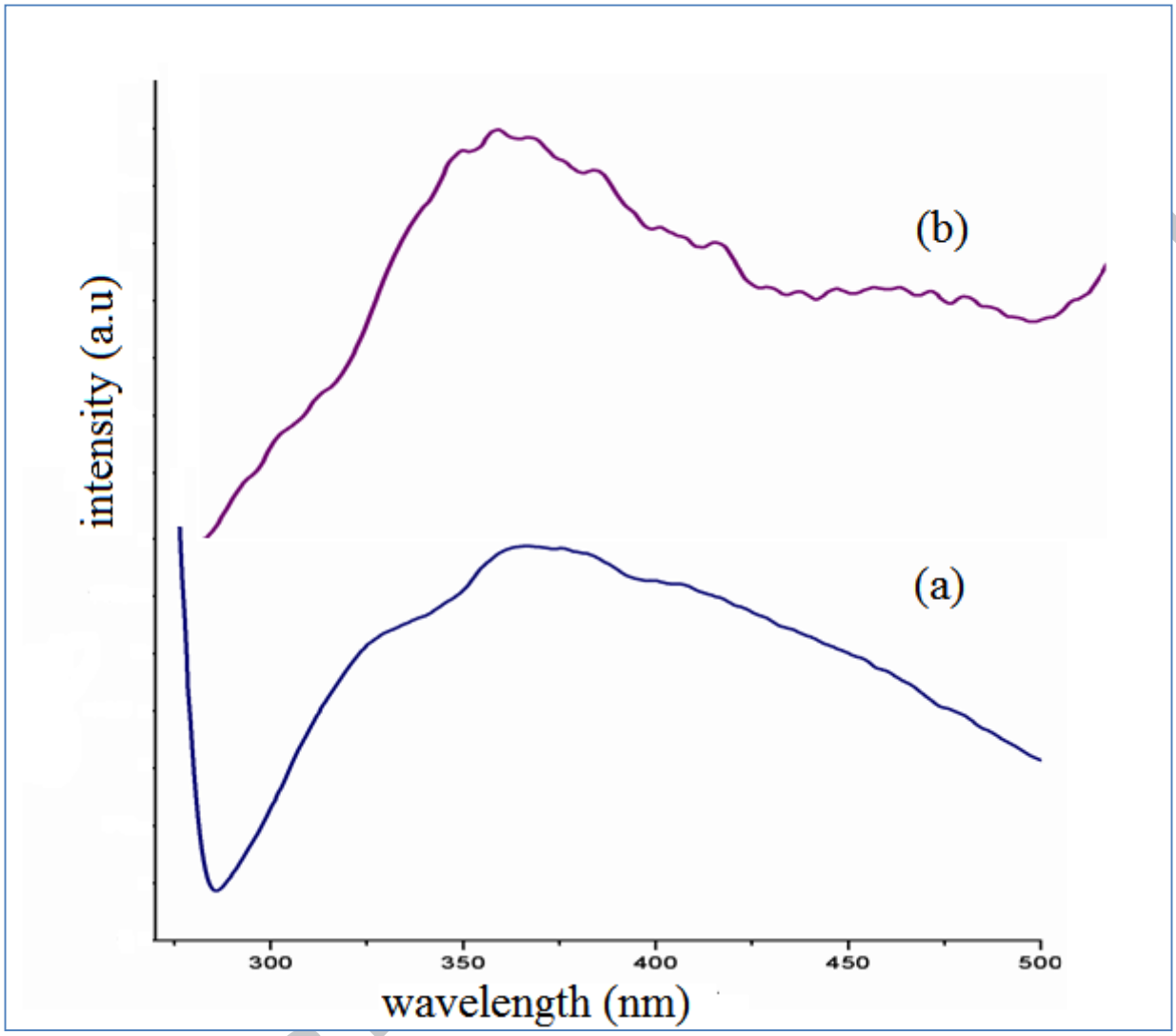

Figure 10.

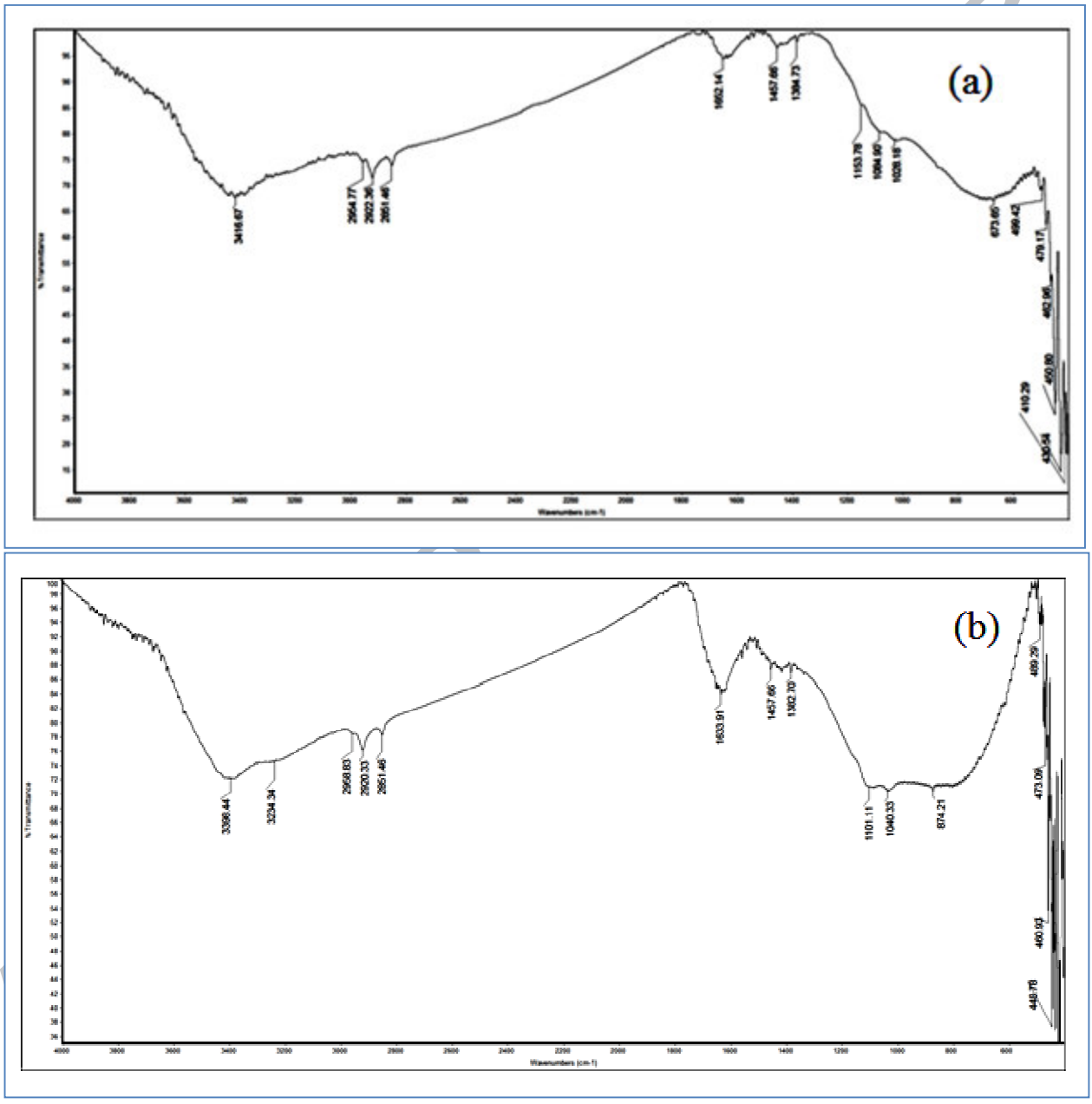

Figure 11.

Graphical abstract (synopsis)

Two Hg(II) dithiocarbamate complexes were prepared and characterized. Complexes **1** and **2** are monomer and polymer, respectively and the geometries around each mercury atom in **1** and **2** are distorted tetrahedral and octahedral, respectively. Complexes **1** and **2** were used as single source precursors for the preparation of α-HgS and β-HgS nanoparticles.

Graphical abstract